40.EAN
40. MEZINÁRODNÍ KONFERENCE EXPERIMENTÁLNÍ ANALÝZY NAPĚTÍ
40th INTERNATIONAL CONFERENCE EXPERIMENTAL STRESS ANALYSIS
3. – 6. VI. 2002, PRAHA/PRAGUE, CZECH REPUBLIC

RATCHETING BEHAVIOR OF CS 1026 STEEL UNDER CYCLIC COMPLICATED BIAXIAL LOADING PATHS

Liliana Blaj

Georges Cailletaud

Abstract

In many engineering applications, structures can be subjected to the action of cyclic loads, which induces repeated yielding. This can lead to degradation and failure of such structures due to the accumulation of deformation (ratcheting).

For describing the ratcheting behavior of Cs 1026 steel, the constitutive model 2M1C (two mechanisms- two kinematic variables, one criteria for defining the elastic domain) is used. The model's parameters were calibrated using uniaxial ratcheting experiments of Hassan and Kyriakides, and a good prediction was obtained using this model. In a previous paper was shown that using the same values for the parameters, acceptable good prediction can be obtain for biaxial simple loading paths.

New experiments of Corona, Hassan and Kyriakides, with complicated biaxial loading paths are used here for a further investigation of model's possibilities. The conclusion is that the simulations obtained for these loading paths are not in good agreement with experiments. This is due to the hardening rule accepted initially for the uniaxial experiments.

Keywords: yield, hardening law, ratcheting, constitutive model, biaxial loading paths, simulations

1. Introduction

The purpose for the present work is to establish whether the constitutive model 2M1C, verified before for the prediction of uniaxial ratcheting and simple paths in biaxial ratcheting behavior, can also give good predictions for complicated loading paths in biaxial experimental loading.

A large number of experiments performed by Hassan and Kyriakides were used as the experimental support.

The classical experiment for obtaining biaxial loading is that in which a thin walled tube with internal pressure is cycled axially in a strain symmetric fashion. This results in progressive increase of the diameter of the tube. (ratcheting in circumferential direction (ε_θ). The rate of this ratcheting depends on the internal pressure applied and the amplitude of the strain cycles used.

2. Experimental procedure

2.1 Uniaxial cycling experiments

The extensive experimental work of Hassan and Kyriakides [1] on CS 1026 carbon steel is used here in order to verify the prediction possibilities of the 2M1C model [2] concerning ratcheting behavior. The uniaxial ratcheting behavior was observed in stress control unsymmetric cycling of CS 1026 carbon steel specimens. The experiments reported in [1] were performed in a closed loop servo- hydraulic test facility. All the specimens were initially tested in the strain range of $\pm$ 1% until they become cyclically stabilized, with a rate of 4 minutes/cycle. Following the strain symmetric cycling, the specimens were unloaded to approximative zero stress and strain and then the test machine was switched to the load control mode and stress control cycling was commenced. The ratcheting phenomena is obvious, as it is shown in Fig. 1,a.

In the first set of experiments, the mean axial stress (σ_{xm}) was kept constant and the amplitude of the cycle was varied (σ_{xa}). The stress- strain curves obtained for different amplitudes were similar in nature with those presented in Fig.1,a. Using a normalized value $\overline{\sigma_{xa}} = \sigma_{xa} / \sigma_0$, with σ_0 – the yield stress, the influence of the stress amplitude can be seen in Fig.2,a, for a constant value of $\overline{\sigma_{xm}} = \sigma_{xm} / \sigma_0 = 0.16$. Here, the evolution of the maximum (peak) stress of each cycle, ε_{xp}, is presented as a function of the number of cycles, N.

2.2 Biaxial cyclic experiments

The experiments of Corona, Hassan and Kyriakides were conducted on tubular specimens with 25.4 mm, outer diameter and 1.27 mm wall thickness. The specimens were machined, heat-treated and cyclically stabilised by strain- symmetric axial cycling as reported in [3]. Results from history I biaxial loading path are presented in Fig. 3 a,b (inset), involving the cycling of σ_θ. In this loading history (inclined path), the axial strain and the circumferential stress vary in phase. In the case shown in Fig. 3, $\varepsilon_{xc} = 0.5\%$, $\overline{\sigma_{xm}} = \sigma_{xm} / \sigma_0 = 0.24$, $\overline{\sigma_{\theta a}} = \sigma_{\theta a} / \sigma_0 = 0.06$. The strain loops are presented in Fig. 3, a. Fig. 3, b presents the induced stress history. Here, the presence of the mean circumferential stress causes the shift of the loops towards the positive σ_x direction.

The next loading history considered is presented in the inset of Fig. 4, a, b and has crossing branches. It proceeds as follows: starting at the point $(\varepsilon_x, \sigma_\theta) = (0, \sigma_{\theta m})$, both ε_x and σ_θ increase to the point $(\varepsilon_{xc}, \sigma_{\theta m} + \sigma_{\theta a})$. Next, ε_x remains constant while σ_θ drops to the value of $(\sigma_{\theta m} - \sigma_{\theta a})$. Following this, ε_x decreases to $(-\varepsilon_{xc})$ while σ_θ increases to $(\sigma_{\theta m} + \sigma_{\theta a})$. In the next step, ε_x remains fixed once more, while σ_θ drops to $(\sigma_{\theta m} - \sigma_{\theta a})$. Finally, ε_x and σ_θ increase simultaneously to return at the starting point of the cycle. Fig. 4 shows results obtained from this loading history (II) for the following cycle parameters: $\varepsilon_{xc} = 0.5\%$, $\overline{\sigma_{xm}} = \sigma_{xm} / \sigma_0 = 0.24$, $\overline{\sigma_{\theta a}} = \sigma_{\theta a} / \sigma_0 = 0.06$. In this case, the circumferential strain has two contributions. It is seen to vary during both of the inclined branches of the cycle when the pressure is increasing and ε_x is varying. In particular, circumferential strain is accumulated in the second halves of these two branches of the cycle, when plastic loading takes place. During the vertical branches of the cycle, the pressure is decreasing while the axial strain is kept at ε_{xc}. As a result, the circumferential strain at $\pm\varepsilon_{xc}$ is seen to decrease. The next effect of these two contributions is still ratcheting in the positive ε_θ direction. The stress history induced by this cycling path is seen in Fig. 4, b to be significantly different from those in Fig. 3, b, and an important difference is that it is only symmetric about some value of σ_x.

3. Comparison of the experimental and predicted ratcheting rates

3.1 Uniaxial ratcheting

Considering the material as cyclically stable after the cyclic symmetric loading applied at the beginning, a constant isotropic hardening law was introduced. In order to simulate the experiments presented in Fig. 1,a, the set of material parameters was established, with $\sigma_0 = 131$ MPa. The simulations were performed with the constitutive equation driver Z.Sim in Z.Set / ZeBuLoN code. The stable hysteresis loop and the following cycles are presented in Fig 1,b. The uniaxial strain is denoted by eto11 and sig11 is the uniaxial stress (σ_x). The stress was varied between 280 and –190 MPa, as in the experiments from [1] (1 ksi = 6.8935 MPa). The predicted accumulated strain is in very good agreement with the experiment, for the same number of cycles, and has in both cases the value of 0.026 (2.6%).

Using the same set of parameters, the maximum strain evolution with the number of cycles was simulated for the same mean stress and various stress amplitudes. The results are presented in Fig. 2, b. A good agreement with the experiment is obtained, mostly for the stress amplitudes of 0.771 and 0.778.

For the simulations for constant stress amplitude of 0.79 and various mean stresses also good predictions are obtained.

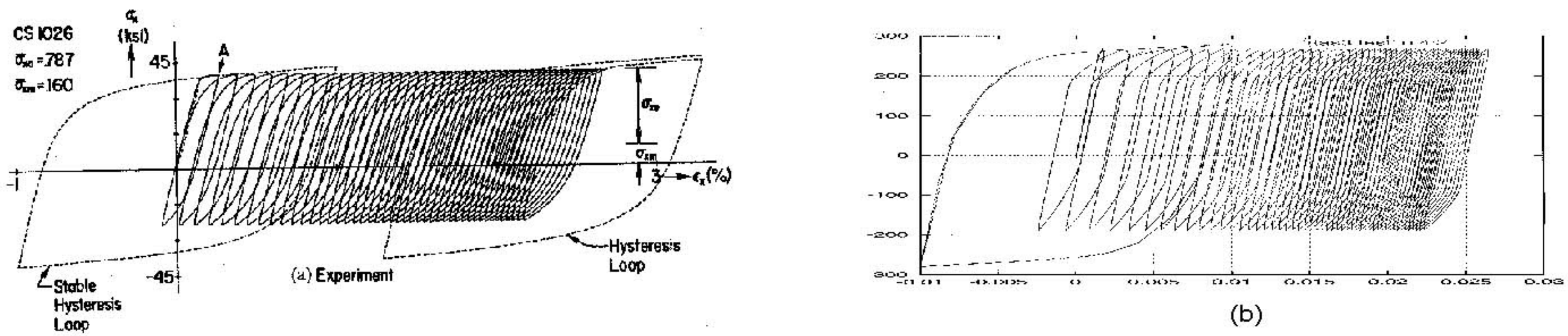

Fig. 1 a, b

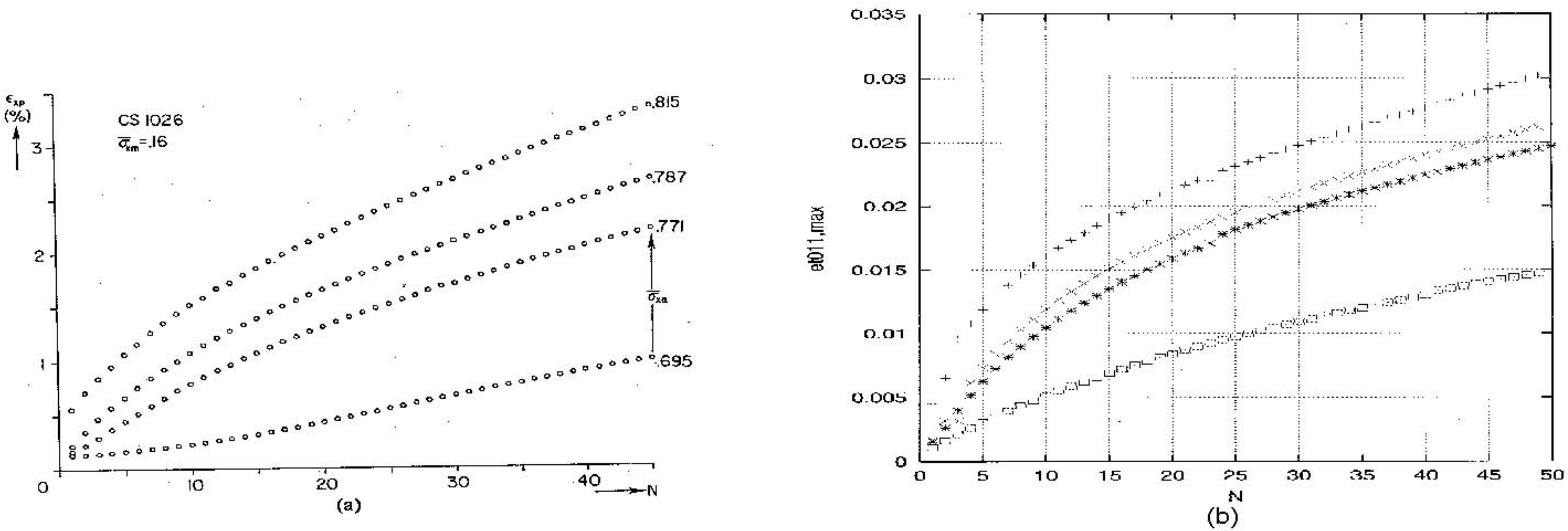

Fig. 2 a, b

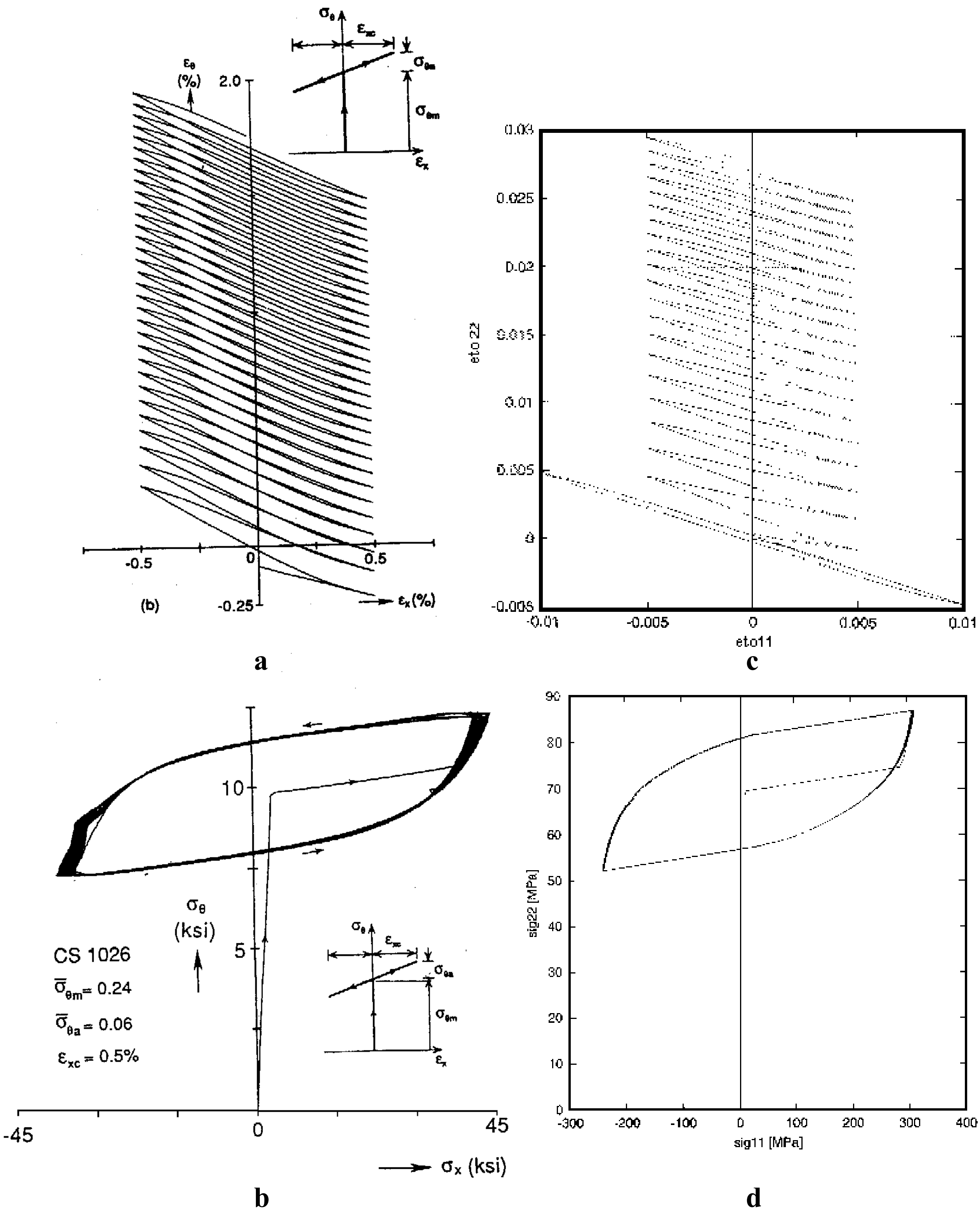

a
b
c
d
CS 1026
$\bar{\sigma}_{\theta m}$= 0.24
$\bar{\sigma}_{\theta a}$= 0.06
ε_{xc} = 0.5%
σ_θ (ksi)
σ_x (ksi)
ε_θ (%)
ε_x(%)
(b)
eto11
eto22
sig11 [MPa]
sig22 [MPa]

Fig. 3 a, b, c, d,

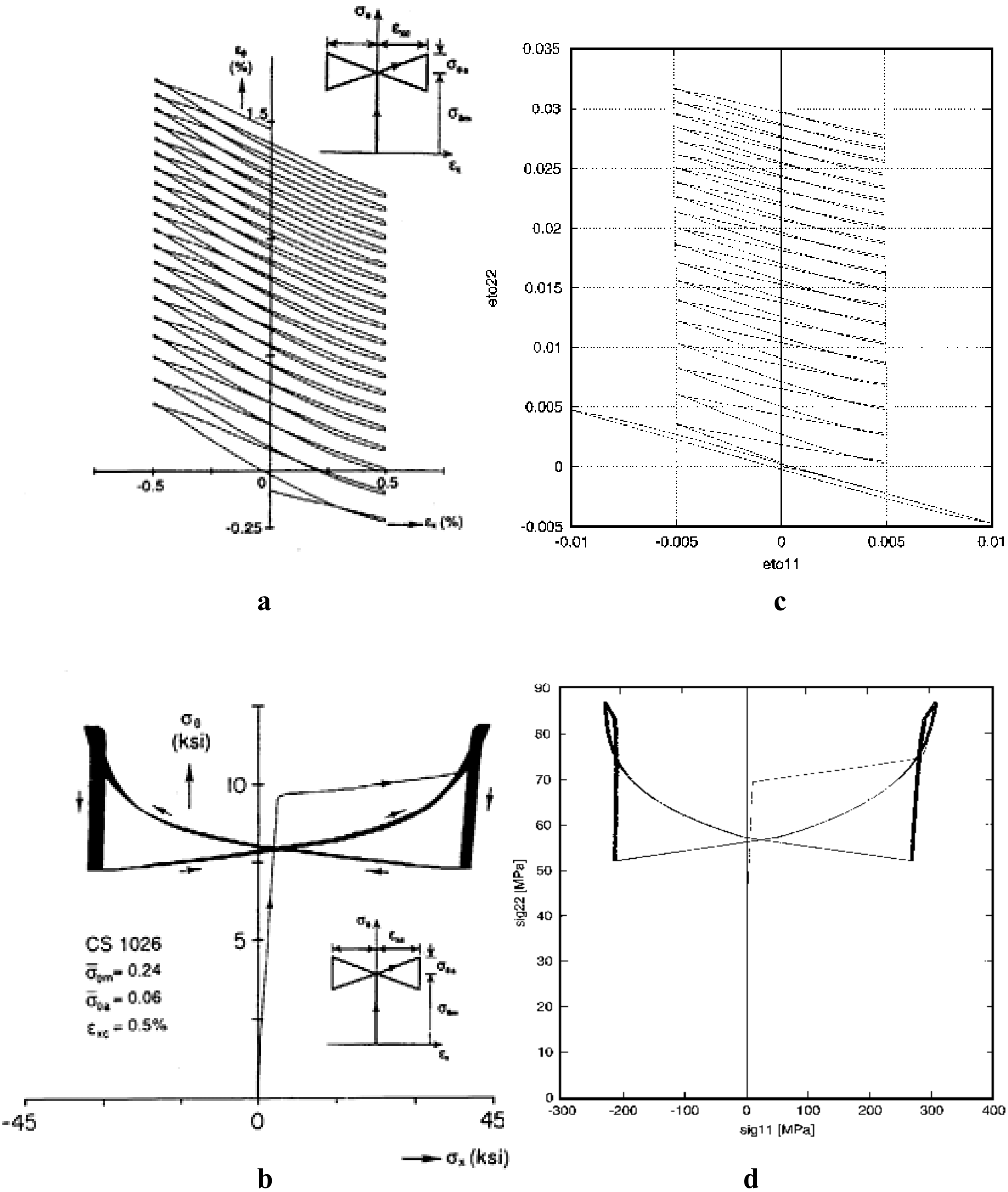

Fig. 4 a, b, c, d,

3.2 Biaxial ratcheting

As we can observe in Fig. 3, a, after 30 cycles the accumulation of circumferencial ε_θ strain is 2%, and the simulation of the same experiment (2M1C constitutive model, with the same set of parameters), for 20 cycles, gives for ε_θ an accumulation of 0.028 (2.8%), much exaggerated comparing with the experiment from Fig. 3, c The circumferential strain (ε_θ) is denoted by eto22 and sig22 is the circumferential stress. Regarding σ_θ versus σ_x representation for the same stress history (Fig. 3, d), the prediction is in good agreement.

Referring to Fig. 4, a, it can be seen that in this experiment, after 20 cycles, the accumulation of ε_θ is 1.75%. The prediction of the same experiment (Fig. 4, c), for the same number of cycles gives 0.03 (3%). This loading history is better simulated then the previous one but still exaggerates the ratcheting behavior. In stress space (Fig 4, d), a good prediction is obtained for the experimental loops from Fig. 4, b.

4. Concluding remarks

The ratcheting rate obtained by the predictions with the 2M1C model is in good agreement with the uniaxial experiments, even if many authors recognize that simulating the ratcheting behavior in cyclic loading is a difficult task.

The comparison between the experiments and the predictions are not in good agreement for the biaxial ratcheting behavior of CS 1026 carbon steel, as the same set of parameters was used as for the prediction of uniaxial ratcheting behavior. The overall allure of the predicted curves and the rate of ratcheting are almost the same as in the experiments, but the accumulation of strain in eto11 and eto22 direction is exaggerated. The changes observed in the sig11- eto11 loops in these cyclic biaxial experiments is larger that in the uniaxial experiments. It was observed that under biaxial cyclic loading, materials exhibit a more important hardening than that observed under uniaxial cyclic. An explanation for these phenomena is given by Wood and Bendler [4], who established that for biaxial cyclic loading (tension and cyclic torsion), the material experiences an accelerated enlargement of slip zones previously activated by the monotonic loading. A study [5] concerning the microstructural examination established differences in the microstructure of the material (304 stainless steel) in uniaxial or biaxial strain cyclic conditions. The main conclusion, affecting macroscopical modeling is that biaxial cyclic loading alters fundamental material features and so, multiaxial experiments are necessary for a more complete representation of a material behavior and a calibration experiment is necessary whenever a new loading history is encauntered.

References

[1] Hassan, T., Kyriakides, S., "Ratcheting in cyclic plasticity", Part I: uniaxial behavior", International Journal of Plasticity, vol.8, 1992, pp 103-116
[2] Cailletaud, G., Sai, K., "Study of plastic/viscoplastic models with various inelastic mechanisms", International Journal of Plasticity, vol. 11, no.8, 1995, pp 991- 1005
[3] Corona, E., Hassan, T., Kyriakides, S.,"On the performance of kinematic hardening rule in predicting a class of biaxial ratcheting histories", International Journal of Plasticity , vol. 12, no. 1, 1996, pp. 117-145
[4] Wood, W. A., Bendler, H. M., "Effect of superimposed static tension on the fatigue behavior in copper subjected to alternating torsion", Transactions of the Metallurgical Society, 17, 1962, p.18-29
[5] McDowell, D. L., "Biaxial path dependence of deformation substructure of type 304 stainless steel", Metallurgical Transactions, 19 A, pp 1227- 1238